JANUARY 1981 PPPL-1738
UC-20g

LIMITING BETA OF STELLARATORS WITH NO NET CURRENT

BY

H. R. STRAUSS AND D. A. MONTICELLO

PLASMA PHYSICS LABORATORY

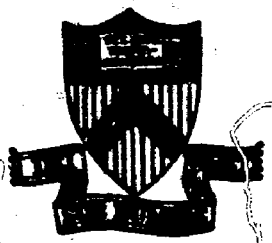

PRINCETON UNIVERSITY
PRINCETON, NEW JERSEY

This work was supported by the U.S. Department of Energy Contract No. DE-AC02-76-CHO 3073. Reproduction, translation, publication, use and disposal, in whole or in part, by or for the United States government is permitted.

Limiting Beta of Stellarators with no Net Current

H. R. Strauss* and D. A. Monticello

Plasma Physics Laboratory, Princeton University

Princeton, New Jersey 08544

* Courant Institute, for Mathematical Sciences, New York University

New York, New York 10012

ABSTRACT

Using reduced nonlinear MHD equations, we find finite beta, resistive, $\ell = 2$ stellarator equilibria with no net current. We then investigate stability to low mode number internal MHD modes, and find beta limits comparable to tokamaks. Low shear equilibria appear to be substantially more stable than high shear.

I. INTRODUCTION

An important advantage of stellarators over tokamaks, is the possibility of steady-state operation. The stellarator rotational transform is then supplied by external windings, rather than by plasma currents which are subject to resistive decay. Even with only a few percent beta, a steady-state device may be economically viable as a fusion reactor. It is nevertheless desirable to attain the highest possible beta.

These considerations motivate the present study. We have solved numerically, reduced equations describing nonlinear, resistive, magnetohydrodynamic motion in stellarators. We have obtained finite beta equilibria, having no net plasma current, consistent with finite resistivity. We have concentrated on $\ell = 2$ stellarators similar to the low shear Wendelstein VII experiment, which has operated with no net current, and to the Heliotron E, which has much higher shear.

Having obtained equilibria, we examine stability to ideal MHD (non-resistive) modes, for toroidal mode numbers $n = 1,2$, and 3. We find an important difference between low and high shear. In both cases, we obtain critical betas comparable to tokamaks, but in the low shear case, there is an accessible upper stable region, suggesting that much higher beta is possible. In high shear $\ell = 2$ stellarators, there is a strongly unfavorable average curvature which overcomes the stabilizing magnetic well.

II. REDUCED STELLARATOR EQUATIONS OF MOTION

The reduced equations are based on the ordering, and methods, of Johnson et al.[1] and Greene and Johnson.[2] These equations are similar to those derived for the high beta tokamak[3] but contain extra terms for the stellarator

rotational transform and field line curvature. A full derivation of the stellarator equations used in this paper has been given by Strauss.[4]

We work with a toroidal coordinate system (r, θ, ζ) where (r, θ) are polar coordinates in the poloidal plane and ζ is the toroidal angle. The major radius is $R = R_o + r \cos\theta$, with $r < a$. We assume the inverse aspect ratio $\varepsilon = a/R << 1$. (In practice, $\varepsilon \lesssim 0.1$.) We assume moderate beta, $\beta \sim \varepsilon$.

The magnetic field, in the lowest order approximation, consists of a constant toroidal field of strength B_o. Added to this is the stellarator field of order

$$\delta = \varepsilon^{1/2}$$

derived from the scalar potential

$$\phi = B_o \sum_{\ell,k} (b_{\ell k}/kh)\, I_\ell(khr) \sin(\ell\theta + k N\zeta + \ell\theta_{\ell k}) \qquad (1)$$

where $I_\ell(x)$ is a Bessel function of imaginary argument: $I_\ell(x) \sim x^\ell$, $x << 1$; $b_{\ell k}$, $\theta_{\ell k}$ are constants, and the stellarator wave length is

$$h = N/R_o \,. \qquad (2)$$

In order ε, the toroidal magnetic field contains corrections from its R^{-1} variation and the diamagnetic pressure balance. Also in this order, we find the poloidal field derived from the toroidal plasma current which we represent as the curl of the toroidal component of the vector potential A_ζ. Hence, through order δ^2, the magnetic field is

$$B = B_o \hat{\zeta} + \delta \nabla\phi - \delta^2 B_o (r/R_o \cos\theta - p/B_o^2) \hat{\zeta}$$

$$+ \zeta^2 \nabla A_\zeta \times \hat{\zeta} . \qquad (3)$$

However, this is not the most useful representation. The stellarator field contains a rapid ζ variation, with $N \gg 1$ fundamental periods in the torus. We assume

$$N \sim \varepsilon^{-1}$$

which implies $h \sim a^{-1}$. We are primarily interested in much longer toroidal wavelengths, with mode numbers $n = 0, 1, 2 \ldots$, such that $n \ll N$. Hence we average over the rapidly varying stellarator field. For example, consider solving

$$B \cdot \nabla\psi = J .$$

We assume $\psi = \psi(r,\theta,\zeta_N,\zeta_n)$, where ζ_N, ζ_n represent the fast and slow toroidal variations, respectively, and

$$\frac{\partial}{\partial\zeta} = \frac{\partial}{\partial\zeta_N} + \delta^2 \frac{\partial}{\partial\zeta_n} .$$

Expanding $\psi = \psi_o + \delta\psi_1 + \ldots$, and using (3), we solve order by order. In $O(\delta^o)$, we have

$$\psi_o = \psi_o (r,\theta,\zeta_n)$$

which means ψ_o has no rapid ζ_N variation. In order $O(\delta)$, we solve

$$(B_o/R_o)\ \partial\psi_1/\partial\zeta + \nabla\psi_o\cdot\nabla\phi = 0 \tag{4}$$

so that ψ_1 is proportional to the stellarator field. In order $O(\delta^2)$, we average over ζ_N, and we can write the result in terms of the averaged magnetic field $\bar{B}$:

$$\bar{B}\cdot\nabla\psi_o = 0$$

where $\bar{B}$, ψ_o depend only on (r,θ,ζ_a).

Applying this method, we obtain the averaged, reduced, nonlinear equations of motion

$$\frac{\partial A}{\partial t} = \bar{B}\cdot\nabla\ u + \eta\ \nabla^2\ A \tag{5}$$

$$\rho_o\ \frac{d}{dt}\ \nabla^2\ u = \bar{B}\cdot\nabla\ \nabla^2\ A + \nabla\ \Omega \times \nabla p\cdot\hat{\zeta} \tag{6}$$

$$\frac{dp}{dt} = 0 \tag{7}$$

where

$$\bar{B}\cdot\nabla = \partial/\partial\zeta + \nabla\Psi \times \hat{\zeta}\cdot\nabla \tag{8}$$

$$\frac{d}{dt} = \frac{\partial}{\partial t} + \nabla\ u \times \hat{\zeta}\cdot\nabla \tag{9}$$

$$\psi = A + \psi_v \tag{10}$$

$$\Omega = 2(r/a)\cos\theta + \Omega_v \tag{11}$$

$$\psi_v = (1/2h\varepsilon) \sum_{\ell,m,k} b_{\ell k}\, b_{mk}\, F_{\ell m}(khr)\cos[(\ell - m)\theta] \tag{12}$$

$$\Omega_v = (1/2\varepsilon) \sum_{\ell,m,k} b_{\ell k}\, b_{mk}\, G_{\ell m}(khr)\cos[(\ell - m)\theta] \tag{13}$$

and where

$$F_{\ell m}(x) = (m/x)\, I'_{\ell}(x)\, I_m(x) \tag{14}$$

$$G_{\ell m}(x) = I'_{\ell}(x)\, I'_m(x) + (\ell m/x^2 + 1)\, I_{\ell}(x)\, I_m(x)\ . \tag{15}$$

We have introduced dimensionless variables, expressing r in units of minor radius a, t in units of poloidal Alfvén time $\rho_o^{1/2} R/B$, A and ψ in units of $\varepsilon a B_o$, and pressure in units of εB_o^2. In these units, $\beta = 2\varepsilon p$. The density ρ, taken constant, is normalized to unity, and $a = 1$.

The variables ψ, A, u, p appearing in these equations are averaged quantities, which are independent of z_N. The stellarator field gives rise to the "vacuum" flux ψ_V, and the field line curvature Ω_V.

If there is no stellarator field, $b_{\ell k} = 0$, the equations reduce to those describing a high beta tokamak.[4]

The stellarator field contributes to the rotational transform, $\iota = 1/q$, through ψ_v:

$$q = 1/\iota = \int d\ell/|\nabla\psi| \tag{16}$$

where the integral is evaluated on a constant ψ surface.

The curvature term Ω_V is generally unfavorable for stability. It persists even in the absence of toroidal curvature and can drive interchange modes. It has been shown[5] that Ω_V is related to the quantity V".

In this paper, we will assume the plasma is in contact with a rigid conducting wall. We choose boundary conditions $\psi = u = 0$. The wall is circular in zero order. The shape of the wall in $O(\delta)$ can be found from (1), (4) and is given by

$$r/a = 1 + \sum_{\ell,k} \Delta_{\ell k} \sin(\ell\theta + k\, N\, \zeta) \tag{17}$$

$$\Delta_{\ell k} = (b_{\ell k}/ha)\, I'_{\ell}(kha). \tag{18}$$

In the following, we will limit consideration to stellarator fields having only one harmonic ℓ,k. We henceforth set $k = 1$ and drop k as a subscript.

Prescribing the boundary shape determines ℓ, N, h, and b_ℓ, which determines the stellarator field. We prefer to specify ℓ, N, h, and ι_a, where ι_a is the vacuum rotational transform at $r = a = 1$. In terms of ι_a, ψ_v, and Ω_v are given by

$$\psi_v = (\iota_a/F'_{\ell a})\, F_{\ell\ell}(hr) \tag{19}$$

$$\Omega_v = 2ha(\iota_a/F'_{\ell a})\, G_{\ell\ell}(hr) \tag{20}$$

where

$$F'_{\ell a} = \partial F_{\ell\ell}(hr)/\partial r,\ r = 1. \tag{21}$$

For small h, we have

$$\psi_v = \frac{1}{2}\,[\iota_a/(\ell-1)]\ r^{2(\ell-1)} + O(h^2) \tag{22}$$

$$\Omega_v = 2h\ \psi_v + O(h^2) \tag{23}$$

$$\Delta_\ell = [\varepsilon\ \iota_a/h(\ell-1)]^{1/2}\ . \tag{24}$$

For small h, an $\ell = 1$ field gives $\iota = 0$; $\ell = 2$ gives $\iota =$ const.; and $\ell = 3$, $\iota \sim r^2$. For $h \gtrsim 1$ an $\ell = 2$ field produces a rotational transform with substantial shear.

From (24), we observe that given ε and ι_a, we cannot make h too small or Δ_ℓ will become too large for our ordering.

III. RESISTIVE EQUILIBRIUM

We are primarily interested in stellarator equilibria consistent with the resistive decay of the plasma current.[6] We seek solutions of Eqs. (5) through (15) with $\partial/\partial\zeta = 0$. Instead of (7), we require $p = p(\psi)$ and $\eta = \eta(\psi)$. This means we are injecting pressure, appropriately, as the plasma evolves. Thus, we solve the two dimensional equations

$$\frac{\partial A}{\partial t} = \nabla u\ x\nabla\psi\cdot\hat{\zeta} + \eta\nabla^2 A \tag{25}$$

$$\frac{d\nabla^2 u}{dt} = \mu\nabla^4 u + \nabla(\nabla^2 A)x\nabla\psi\cdot\hat{\zeta} + \nabla\Omega\ x\ \nabla p\cdot\hat{\zeta} \tag{26}$$

$$P = P_o(\psi/\psi_o)^K \tag{27}$$

where ψ_o is the value on axis. Usually, we choose η = const. Viscosity μ has been added to (26) to dissipate kinetic energy so that an equilibrium can be reached. In equilibrium,

$$\nabla^2 A = -(1/\eta)\ \nabla u \times \nabla\psi \cdot \hat{\zeta}\ . \tag{28}$$

Integrating around a flux surface ψ = const, we have

$$\langle \nabla^2 A \rangle = 0 \tag{29}$$

where the flux surface average of a quantity f is

$$\langle f \rangle = \left[\int d\ell\ f/|\nabla\psi|\right]/\left[\int d\ell/|\nabla\psi|\right] \tag{30}$$

and where $d\ell$ is the arc length. This is the well-known result that a stellarator in resistive equilibrium has no net current on each flux surface.[6]

It follows from (29) that the total current also vanishes. However, locally there must be some current in order to have momentum balance. If the current is given, (28) requires that u is of order η . In equilibrium, u may be neglected in (26) for sufficiently small η , and we may integrate to obtain

$$\nabla^2 A = -\Omega \frac{dp}{d\psi} + g(\psi). \tag{31}$$

This is the equilibrium equation of Greene and Johnson.[2] However, $g(\psi)$ is determined by (29) which gives

$$\nabla^2 A = \left[\langle\Omega\rangle - \Omega\right] \frac{dp}{d\psi} . \tag{32}$$

This is a generalized partial differential equation, as discussed by Grad et al.[7] Methods have been found for solving equations of this type, iterating between solutions of Poisson's equation on the left hand side and the calculation of the flux surface averages on the right hand side. Although we do not employ such methods here, it is important to note that the solutions of such equations, in practice, are unique. Hence specifying ψ_v and $p(\psi)$ serves to determine a generally unique equilibrium, regardless of initial conditions, the form of $\eta(\psi)$, and the magnitude of η and μ , providing η is sufficiently small. This has been verified in our numerical work.

It is instructive to examine the energy conservation law associated with Eqs. (25) - (27). Assuming ψ = u = const. at r = 1, and defining the energy

$$E = \frac{1}{2} \int d^3x \left[(\nabla A)^2 + (\nabla u)^2 - 2\Omega p \right] \tag{33}$$

we obtain

$$\frac{\partial E}{\partial t} = - \int d^3x \left[\eta \nabla^2 A \left(\nabla^2 A + \Omega \frac{dp}{d\psi} \right) + \mu (\nabla^2 u)^2 \right] . \tag{34}$$

The term $\Omega dp/d\psi$ would not appear if there were no pressure sources, i.e., if $dp/dt = 0$. Neglecting $\eta^2 u$, we verify that $\partial E/\partial t = 0$ in equilibrium.

We now present approximate analytic solutions of Eq. (32). Assuming small β and h , we find expressions for the rotational transform and for the

shift of the magnetic axis, assuming a single harmonic stellarator field. Unlike Johnson et. al,[5] we assume ψ = const. on the boundary r = 1. Hence, *we do not find a class of solutions with negative shift of the magnetic axis.* Also with our boundary conditions, we would need to introduce more stellarator harmonics ℓ in order to obtain Scyllac type[8] solutions.

From (14),(20), we obtain for small h,

$$\psi_v = \frac{\iota_a}{2(\ell-1) + h^2} \left[r^{2(\ell-1)} \left(1 + \frac{h^2 r^2}{2\ell}\right) - \left(1 + \frac{h^2}{2\ell}\right) \right] . \qquad (35)$$

We find

$$\iota/\iota_a = \left[\frac{2(\ell - 1) + h^2 r^2}{2(\ell - 1) + h^2}\right] r^{2(\ell-2)} . \qquad (36)$$

We now solve (32) by expanding in β:

$$\psi = \psi_o + \beta\psi_1 + \cdots ,$$

In zero order, $\psi_o = \psi_v(r)$. In first order,

$$\Omega_v p'(\psi_v) + g_1(\psi_v) = 0$$

$$\nabla^2 A_1 + 2r \cos\theta \; p'(\psi_v) = 0 .$$

Consider a pressure profile of the form (27).

If K = 1, $p' = - p_o/\psi_v(0)$. Then

$$A_1 = \frac{P_o}{4\psi_v(0)} (r^3 - r) \cos\theta \ .$$

To find the magnetic axis, we solve

$$\nabla(\psi_v + A_1) = 0 \ .$$

Taking the terms with the lowest powers of r in ψ_v and A, we find that the magnetic axis is located at $r = r_m$, $\theta = 0$, where

$$r_m^{2\ell-3} = \frac{P_o q_a^2}{2} \frac{[i + h^2/2(\ell-1)]^2}{1 + h^2/2\ell} \tag{37}$$

and where $q_a = 1/\iota_a$.

When $\ell = 2$, the displacement of the magnetic axis is proportional to the poloidal beta $\beta_p = \beta q_a^2/\epsilon^2$. When $\ell = 3$, r_m is larger and scales with $(\beta_p \epsilon)^{1/3}$.

IV. NUMERICAL RESULTS

We solve Eqs. (5) through (15) and (26) through (30) numerically using STELLA, a modification of the Princeton high beta tokamak code HIB.[9,10] The equations are Fourier analyzed in the angles θ and ζ, and finite differenced in r. The resulting coupled mode equations are time advanced by a two level predictor corrector method. Convolution sums are performed directly, taking advantage of the vector processing of the MFE CRAY-1 computer. Typically we used 50 radial mesh points, with 6 poloidal harmonics for equilibrium calculations, and 15 poloidal harmonics for stability.

To find equilibria, we start with an initial cylindrical state with $\psi = \psi_v(r)$ and the pressure given by (27). The equations are time advanced until a steady state is reached.

Fig. I shows the constant pressure (and flux) surfaces for an equilibrium with input parameters $\ell = 2$, $ha = 0.25$, $q_a = 1.80$, and $P_o = 0.13$. These parameters correspond to the Wendelstein VII experiment.[11] Recall that in our dimensionless units

$$\beta = 2\varepsilon p.$$

The pressure is quadratic in ψ, $K = 2$. The average pressure is about $0.4\ P_o$. Note the typical finite beta outward shift of the magnetic axis. As mentioned above, more stellarator harmonics would be required for an inward shift; in this case, an additional $\ell = 1$ or $\ell = 3$ field.

Contours of constant toroidal current density are shown in Fig. 2. The separatrix which divides the regions of positive and negative current passes through the magnetic axis as required by Eq. (29). The total current vanishes to an accuracy of about 10^{-3}.

The current profile along the major radius is given in Fig. 3. As in the high beta tokamak, the current exhibits peaking near the outer edge of the plasma. However, the magnitude of the current is substantially less than for a comparable tokamak.

The rotational transform $\iota = 1/q$ is one of the main factors determining stability. The q profile is shown in Fig. 4. Due to the small value of ha, the profile is almost flat. It is noteworthy that the peak value of q occurs at neither the magnetic axis or the wall. These features of the q profile will prove important for interpreting our stability results for equilibria of this type. Note that the safety factor at the wall is not exactly equal to q_a, since q_a refers only to the vacuum field.

For small beta and ha, the shift of the magnetic axis agrees well with Eq. (28), for the linear pressure profile, K = 1. Figure 5 compares the results for parameters $\ell = 2$, $ha = 0.25$, *and* $qa = 1.8$ with r_m, the radial displacement of the magnetic axis, plotted as a function of P_o.

In Fig. 6, we show the q profile of another equilibrium, with input parameters $\ell = 2$, $ha = 1.8$, $qa = 0.555$, $P_o = 0.2$, and $K = 2$. Due to the rather large value of ha, there is substantial shear, and finite beta effects are less important. The contours of p, ψ, and current are qualitatively similar to the low shear $\ell = 2$ case. These parameters correspond to the Heliotron-E[12] experiment, which has $\varepsilon = 0.1$. The magnetic axis shift as a function of P_o is shown in Fig. 7.

We now consider the stability of finite beta, $\ell = 2$ stellarator equilibria with no net current, having parameters consistent with those considered above. To find unstable eigenmodes, the averaged equations of motion (5), (6), (7) are linearized. The equilibrium quantities are independent of ζ, so the eigenmodes have ζ dependence exp $(in\zeta)$. The fastest growing instability for a given equilibrium and toroidal mode number n can be found by integrating the equations in time. We consider only ideal, non resistive modes, with $\eta = 0$ in Eq. (5). We also neglect the equilibrium resistive flow.

We first examine the low shear case, $ha = 0.25$. Figure 8 shows contours of the perturbed velocity potential u, for an $n = 3$ instability of an equilibrium with $q_a = 1.8$, $P_o = 0.13$. Referring to Fig. 4, we note that the mode is concentrated near the flux surface of maximum q, which is close to 2. The dominant poloidal mode number is $m = 6 \approx nq$. It is interesting that there is instability without an exact rational surface in the plasma, since $q < 2$.

Figure 9 shows the squared growth rate in units of the poloidal Alvfen time, as a function of P_o, with parameters $\ell = 2$, ha = 0.25, qa = 1.85. These equilibria have K = 2, which means the pressure is quadratic in ψ. Curves are plotted for toroidal mode numbers n = 2,3. Just as in the high beta tokamak, there is a second stability region due to the magnetic well. The lower critical β is 0.2 ε, which is comparable to a tokamak,[9] but the upper critical β is only 0.4 ε. The growth rate is of order 0.1 $B/\rho_o^{1/2} R$ which is about the same as was found in tokamaks. Hence equilibria of this type have good stability.

At low shear, stability depends critically on the rational surfaces, at which q = m/n. For low n there is only one rational surface in or near the plasma. Recall that in these equilibria, q varies by only a few percent, with the maximum q somewhat larger than q_a. Fig. 10 shows the effect of varying q_a, with $\ell = 2$, ha = 0.25, and $p_o = 0.13$, which corresponds to the middle of the unstable range of Fig. 9. The curves show the growth rate squared for n = 1,2,3 modes, as a function of q_a. For n = 3, there are rational surfaces at q = 1.667, 2.0, 2.333, 2.667, with m = 5,6,7,8. Above the n = 3 curve are shown the dominant poloidal mode number (m) of the most unstable mode. The maximum growth rates are correlated with the minimum values of $|m - nq|$. The results are similar for n = 1 and n = 2.

If we consider modes with n less than or equal to 3, we see that there are especially favorable q values for stability. In Fig. 11 we plot the growth rate squared as a function of β, for $q_a = 1.70$. With this choice of q_a, the n = 1,2,3 modes are completely stable. The mode frequency reaches its minimum at $\beta = 0.4\ \varepsilon$, which is higher than the most unstable β at $q_a = 1.85$.

Of course, for very large n, the rational surfaces become dense, and there should be no gaps in the range of unstable β values. It may be

legitimate to look only at low n, however, if finite Larmor radius effects are important. In any case, a key assumption of the present theory is that n is much less than N, the number of stellarator periods, and typically N is of order 10. Hence large n results would be of dubious validity. In Wendelstein VII, N = 5; in Heliotron E, N = 18.

Turning now to the high shear $\ell = 2$ equilibria, we find a rather different stability picture. We consider parameters $\ell = 2$, ha = 1.80, q_a = 1.80, with a quadratic pressure profile, K = 2. Referring to Fig. 6, we note that there are typically several rational surfaces in the plasma. Figure 12 shows the squared growth rate as a function of β, for n = 1,2,3. The critical $\beta = 0.33\ \varepsilon$. There is no second stability region. This may be understood by recalling from Eq. (20) that the stellarator curvature Ω_v, which is unfavorable, is proportional to ha. Hence it is 7.2 times larger than in the previous low shear case. The stabilizing magnetic well, caused by the outward shift of the magnetic axis, is insufficient to balance the stellarator curvature and produce a second stable region.

Our results suggest that low shear is desirable for $\ell = 2$ finite beta stellarators with no net current, for which ι is chosen to exclude low order rational surfaces from the plasma. However the stellarator wavelength h which governs the shear, may not be made arbitrarily small, if q_a and ε are fixed. As shown by Eq. (24), the outer flux surface distortion can become large, so that our ordering breaks down. Given this constraint, it seems worthwhile to keep ha, and thus the shear and Ω_v, as small as possible. Nonetheless, the high shear $\ell = 2$ stellarator has a critical beta comparable to a tokamak. Add to this the potential for steady-state operation, and the stellarator seems, once again, a reasonable candidate for a future fusion reactor.

ACKNOWLEDGMENT

The authors thank J. L. Johnson, T. K. Chu, P. Garabedian, and O. Betancourt for helpful discussions. One of us (H.S.) thanks P. H. Rutherford and R. C. Grimm for making possible a recent visit to Princeton Plasma Physics Laboratory, where this work was performed.

This research was supported by the United States Department of Energy under contract no. DE-AC02-76-CH03073.

REFERENCES

1. J. L. Johnson, C. R. Oberman, E. M. Kulsrud, and E. A. Frieman, Phys. Fluids 1, 281, (1958).

2. J. M. Greene and J. L. Johnson, Phys. Fluids 4, 875, (1961).

3. H. R. Strauss, Phys. Fluids 20, 1354, (1977).

4. H. R. Strauss, Plasma Physics 22, 733, (1980).

5. J. M. Greene, J. L. Johnson, and K. A. Weimer, Plasma Physics 8, 145, (1966).

6. M. D. Kruskal and R. M. Kulsrud, Phys. Fluids 1, 265, (1958).

7. H. Grad, P. N. Hu, and D. C. Stevens, Proc. Natl. Acad. Sci. USA 72, 3789, (1975).

8. J. P. Freidberg, R. Y. Dagazian, and D. C. Barnes, Phys. Fluids 22, 926, (1979).

9. H. Strauss, W. Park, D. A. Monticello, R. B. White, S. C. Jardin, M. S. Chance, A. M. M. Todd, and A. H. Glasser, Nucl. Fusion 20, 628, (1980).

10. D. A. Monticello, W. Park, S. C. Jardin, M. S. Chance, R. L. Dewar, R. B. White, R. C. Grimm, J. Manickam, H. R. Strauss, J. L. Johnson, J. M. Greene, A. H. Glasser, P. K. Kaw, P. H. Rutherford, and E. J. Valeo, 8th International Conference on Plasma Physics and Controlled Nuclear Fusion Research, I.A.E.A., Brussels (1980).

11. W VII Team, 8th International Conference on Plasma Physics and Controlled Nuclear Fusion Research, I.A.E.A., Brussels (1980).

12. K. Uo, A. Iiyoshi, T. Obiki, S. Morimoto, M. Wakatani, A. Sasaki, K. Kondo, O. Motojima, M. Sato, K. Hanatani, T. Mutoh, H. Zushi, H. Kaneko, I. Ohtake, M. Nakasuga, T. Mizuuchi, S. Kinoshita, and

Y. Nakashimo, 8th International Conference on Plasma Physics and Controlled Nuclear Fusion Research, I.A.E.A., Brussels (1980).

FIGURE CAPTIONS

Fig. 1. Contours of constant ρ (ψ) for a zero net current stellarator equilibrium with $\ell = 2$, ha = 0.25, $q_a = 1.7$, and $\beta = 0.26\ \epsilon$. These parameters correspond to the Wendelstein VII experiment, which has $\epsilon = 0.05$.

Fig. 2. Contours of constant toroidal current density of the equilibrium of Fig. 1. The separatrix, dividing positive and negative current regions, passes through the magnetic axis. The net current on each flux surface vanishes due to Eq. (28).

Fig. 3. Toroidal current profile as a function of r, along the major radius. The current is peaked more in the outer (large R) part of the plasma.

Fig. 4. Rotational transform profile as a function of r along the major radius, for the equilibrium of Fig. 1. Due to the small value of ha, $q(\psi)$ is almost flat. The peak q occurs at neither the magnetic axis nor the plasma boundary.

Fig. 5. Displacement of the magnetic axis as a function of β, for magnetic parameters $\ell = 2$, ha = 0.25, $q_a = 1.8$. The displacement tends to saturate at large beta. At low beta, there is good agreement with Eq. (37), also shown, which gives a displacement linear in beta.

Fig. 6. The q profile of a different equilibrium, with $\ell = 2$, ha = 1.8, $q_a = 0.555$, and $\beta = 0.4\ \varepsilon$. The magnetic field parameters are similar to the Heliotron E experiment, which has $\varepsilon = 0.1$. With large ha, there is substantial shear. The peak q occurs at or near the magnetic axis.

Fig. 7. Magnetic axis shift r_m as a function of $p_o = \beta/2\varepsilon$ for ha = 1.8 equilibria. The solid line is the analytic result for small P_o.

Fig. 8. Contours of perturbed velocity potertial u, of an n = 3 linear eigenmode of an equilbrium with ha = 0.25, $q_a = 1.8$, $p_o = 0.13\varepsilon$.

Fig. 9. Linear stability of equilibria with $\ell = 2$, ha = 0.25, $q_a = 1.85$, as a function of β/ε, and for toroidal mode numbers n = 2,3. There is a high beta stability region due to the magnetic well. The critical (peak) betas are 0.2 ε and 0.4 ε .

Fig. 10. The effect of varying q_a. The squared growth rate is shown for n = 1 (dotted line), n = 2 (dashed line), n = 3 (solid line). Beta is 0.26 ε in the middle of the unstable range of Fig. 8. The dominant poloidal mode number of the most unstable mode is also shown. Instability is correlated with the presence of a rational surface q = m/n in the plasma.

Fig. 11. Growth rate squared as a function of beta, for n = 1,2,3 modes. The equilibria are almost the same as in Fig. 8, except $q_a = 1.7$. This is sufficient to stabilize the modes.

Fig. 12. Stability of equilibria with $\ell = 2$, $\iota a = 1.8$, $q_a = 0.555$. The growth rate squared is shown as a function of beta, for $n = 1,2,3$ modes. The critical beta is $0.33\,\epsilon$, and there is no high beta stability. Unlike the previous low shear case, there are always rational surfaces in the plasma, and the unfavorable stellarator curvature, Ω_v, is much larger.

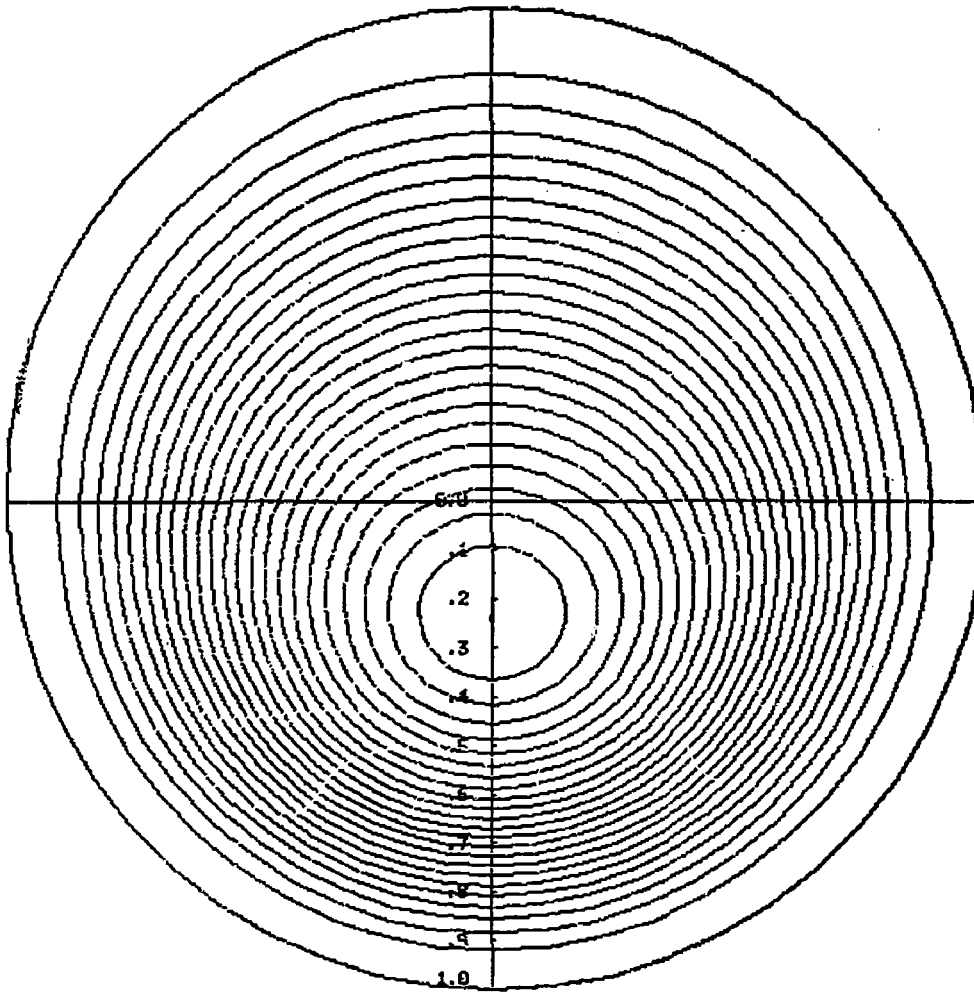

Fig. 1. (PPPL-802320)

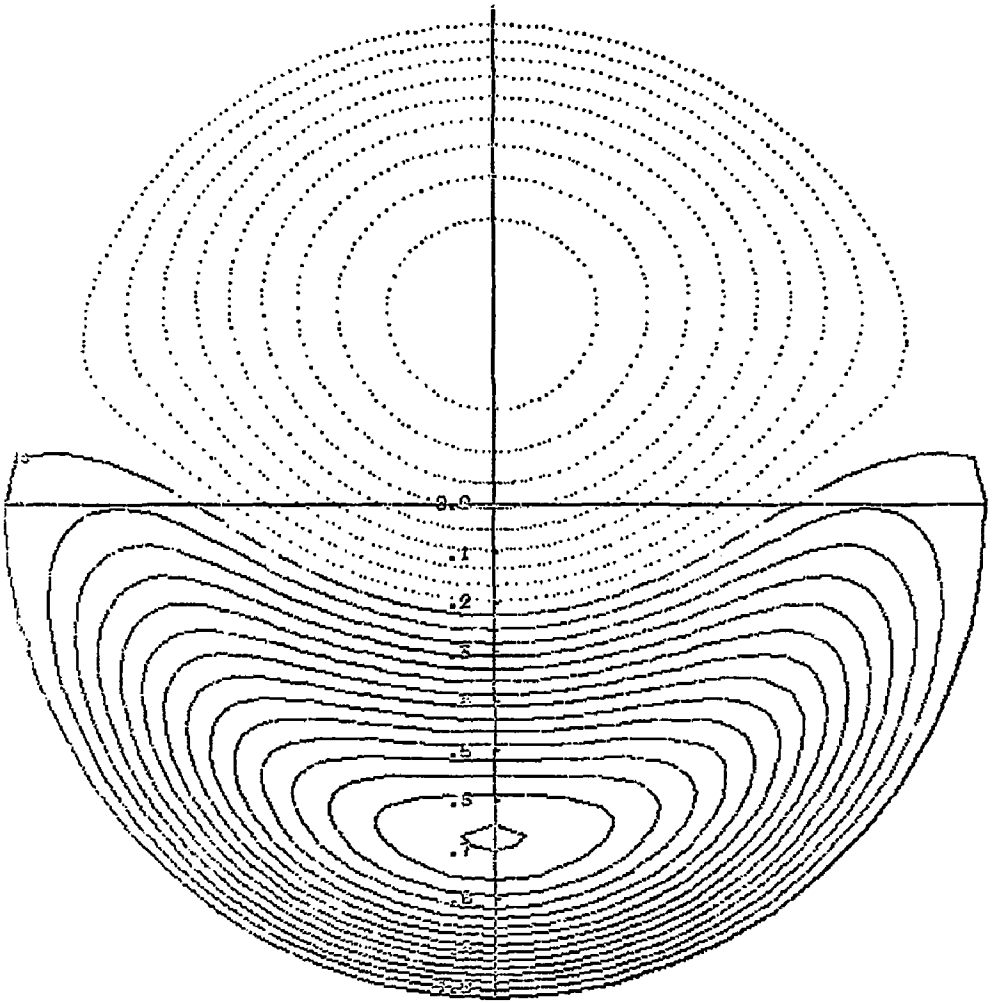

Fig. 2. (PPPL-802318)

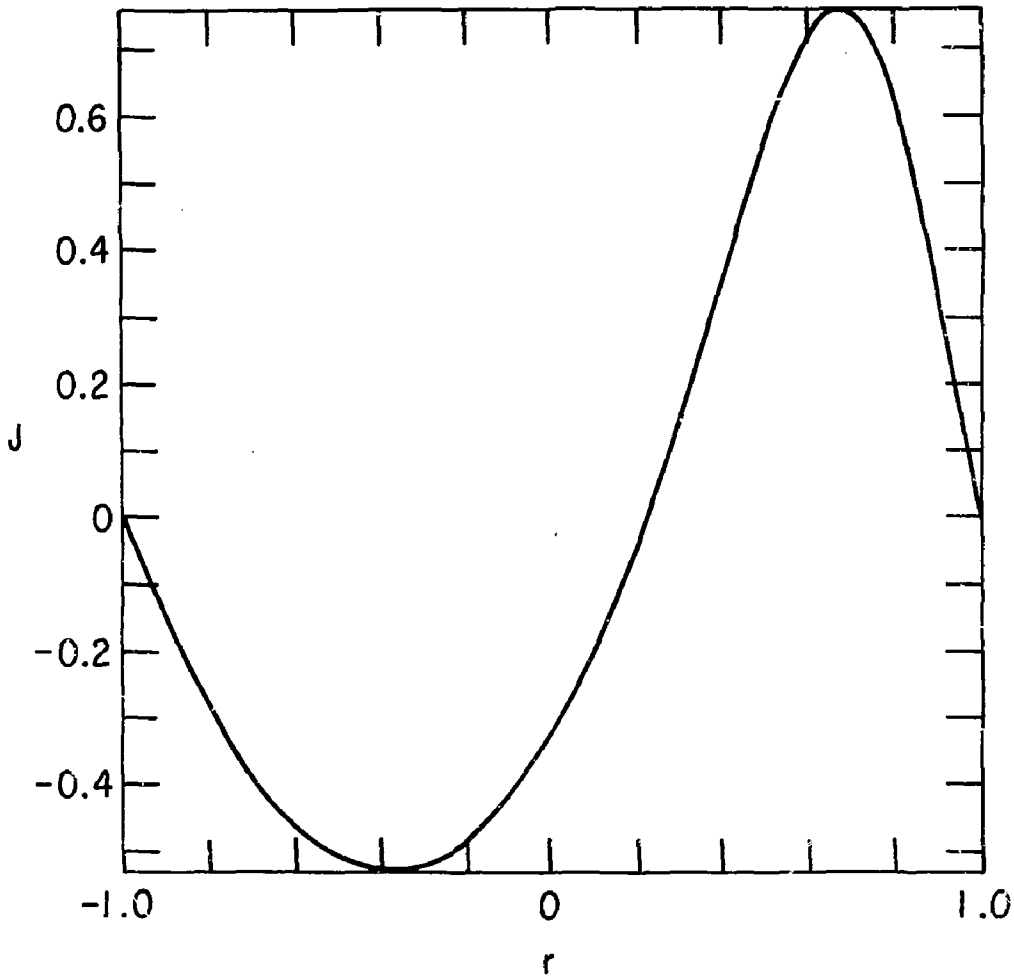

Fig. 3. (PPPL-802333)

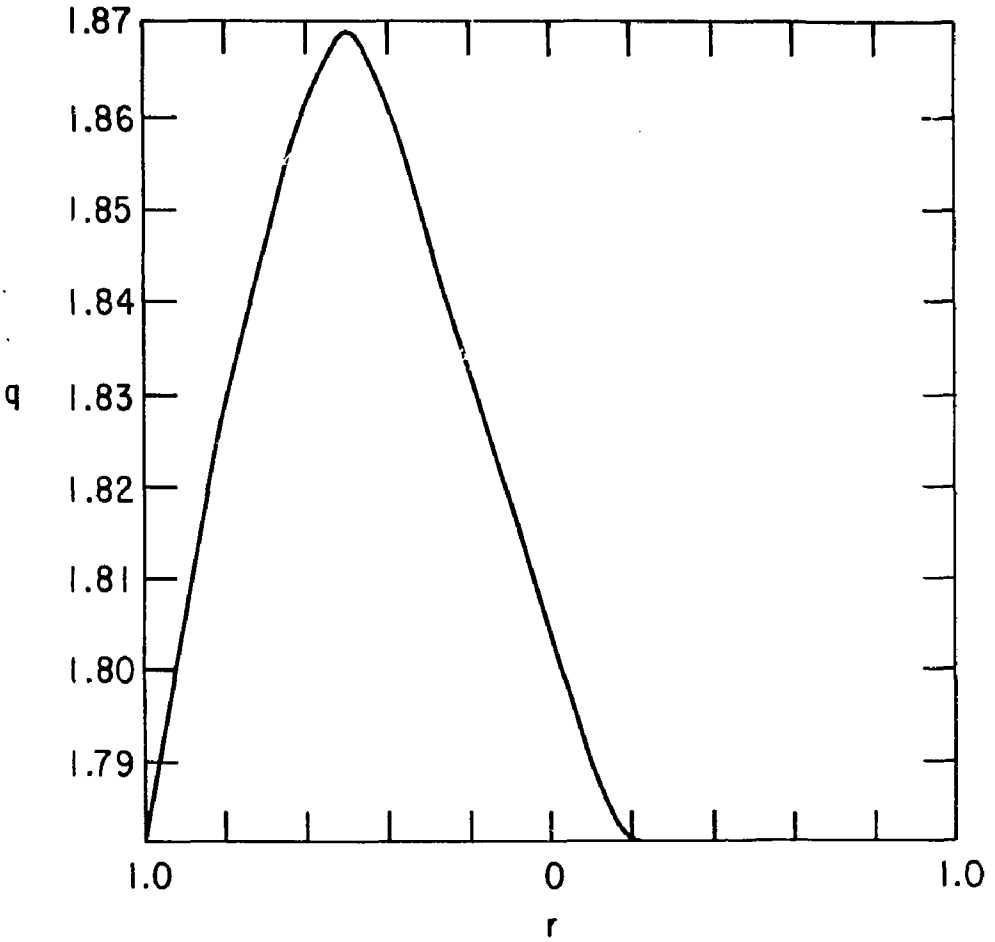

Fig. 4. (PPPL-802412)

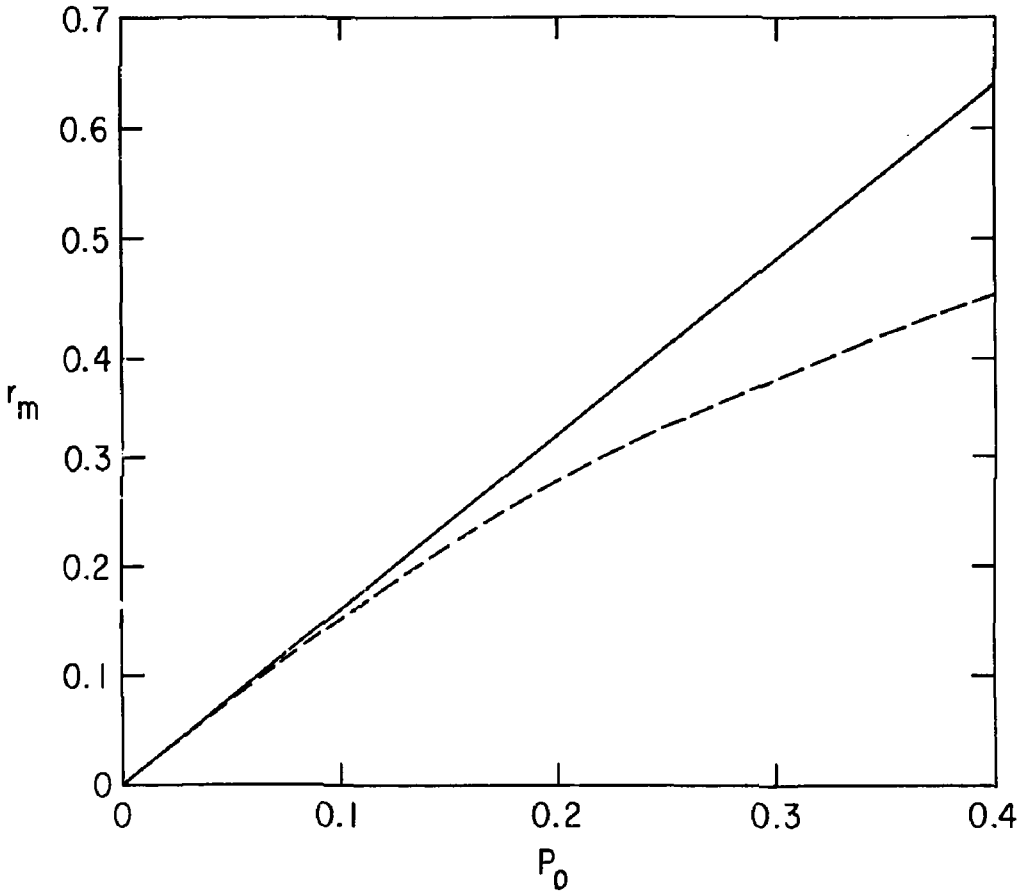

Fig. 5. (PPPL-802331)

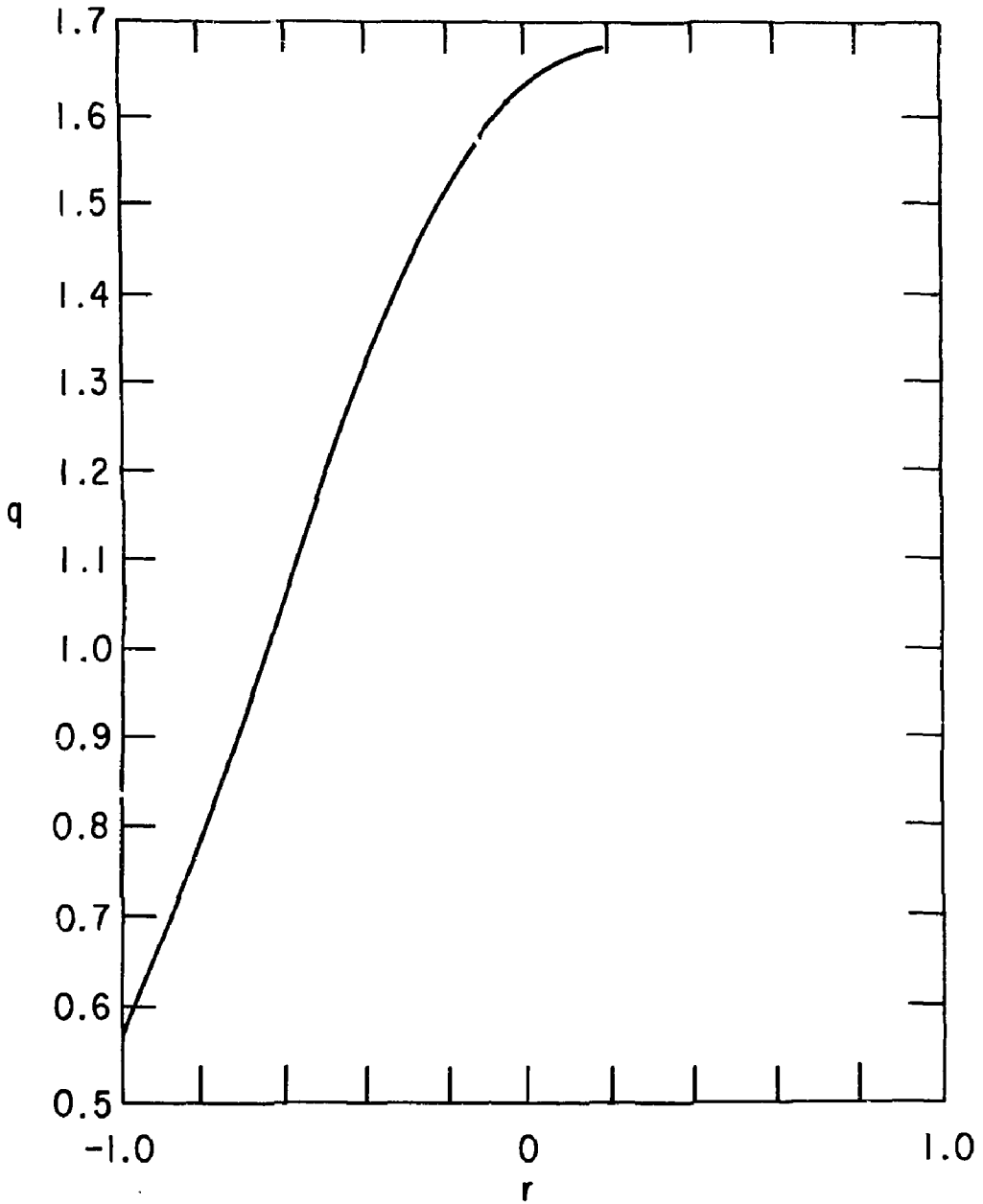

Fig. 6. (PPPL-802332)

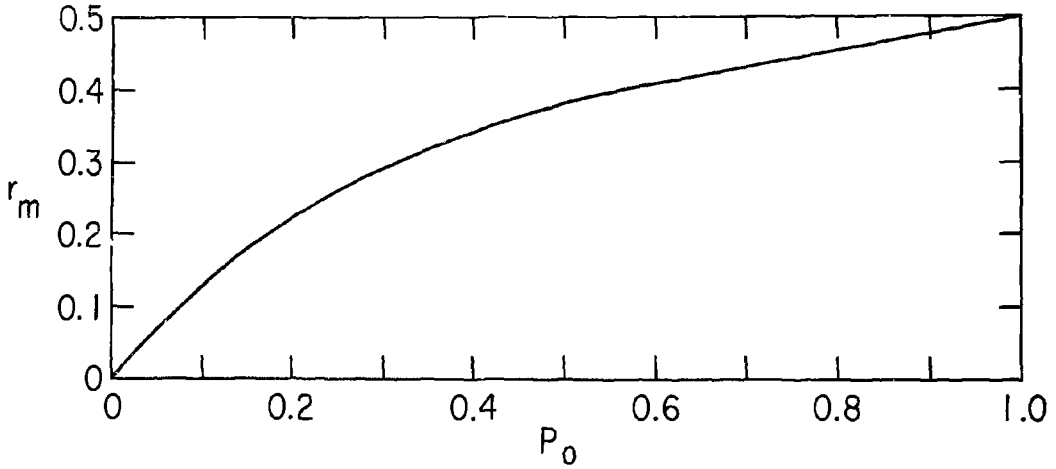

Fig. 7. (PPPL-802409)

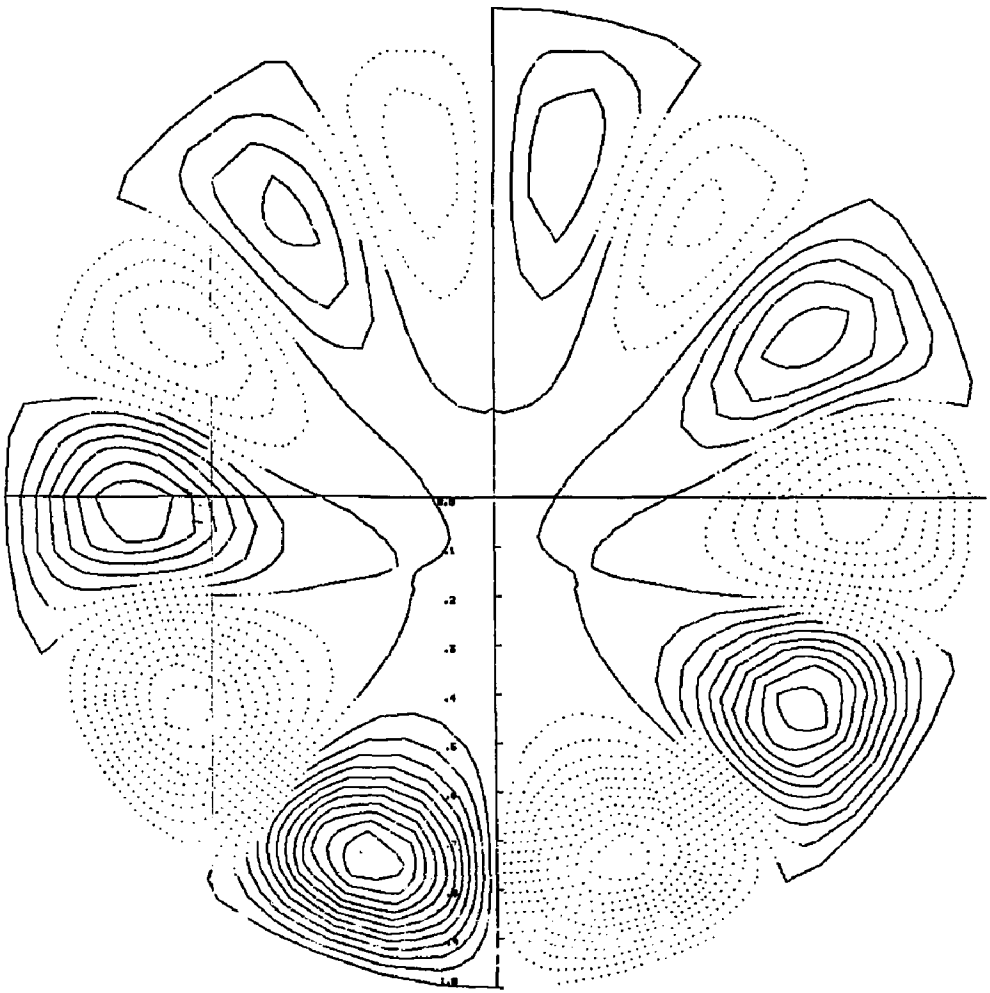

Fig. 8. (PPPL-802321)

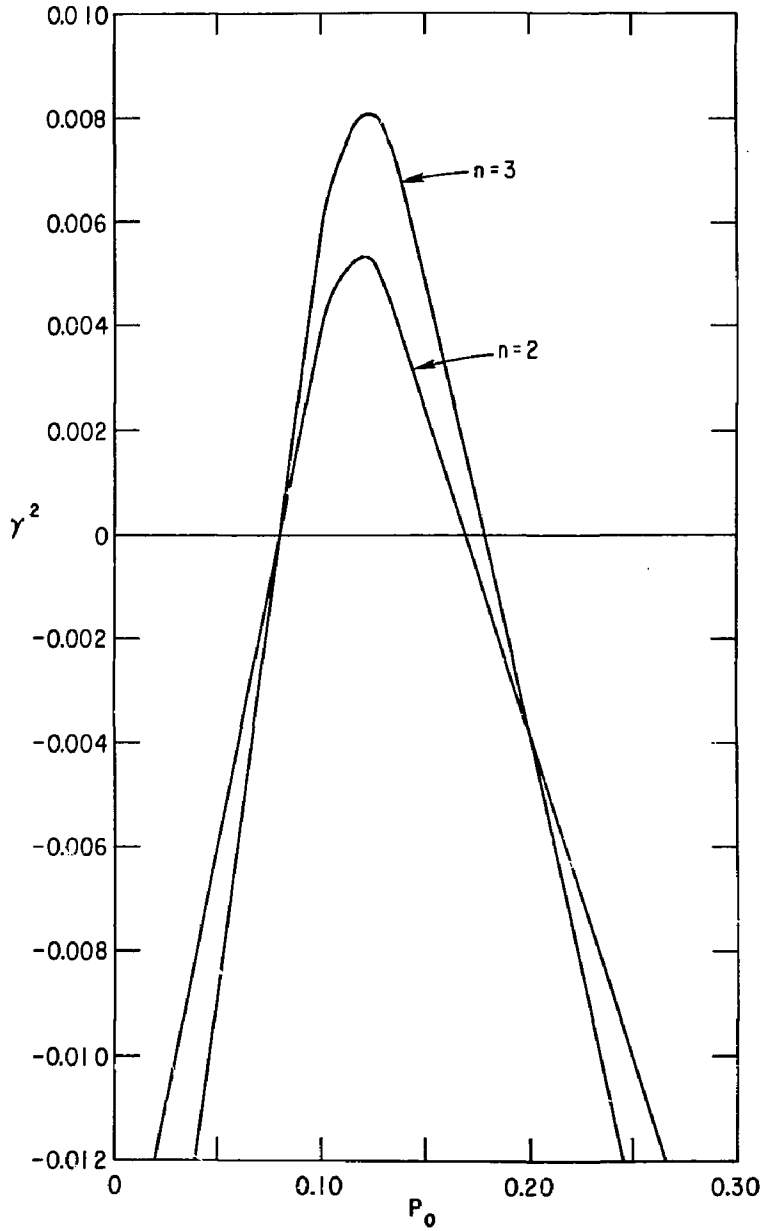

Fig. 9. (PPPL-802413)

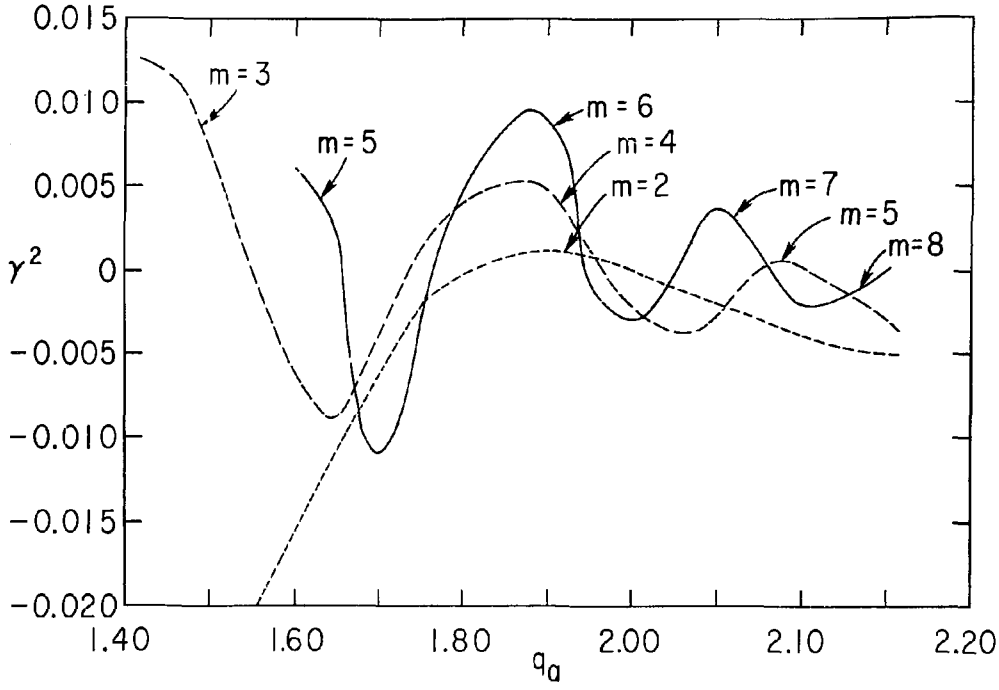

Fig. 10. (PPPL-802410)

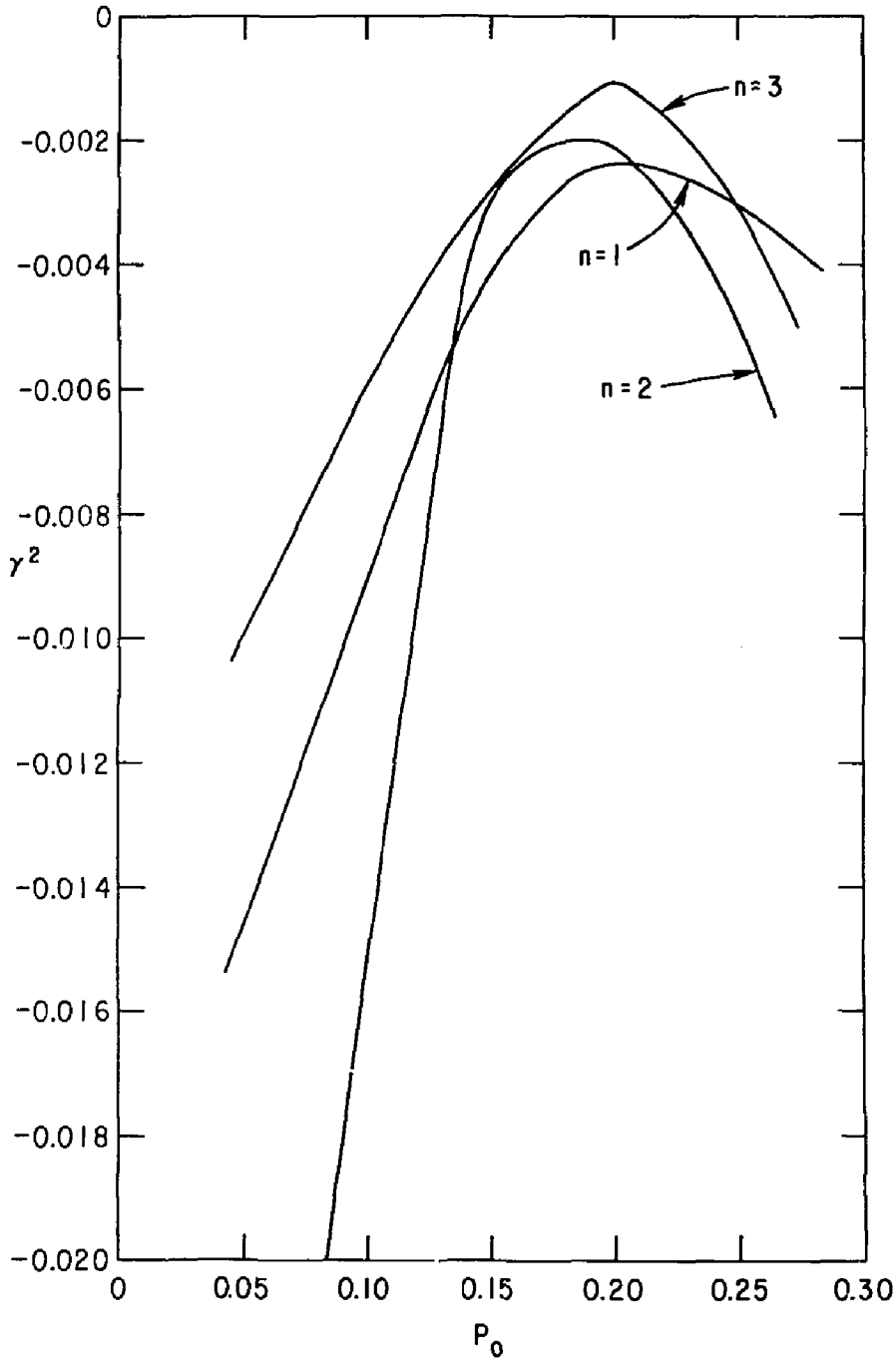

Fig. 11. (PPPL-802414)

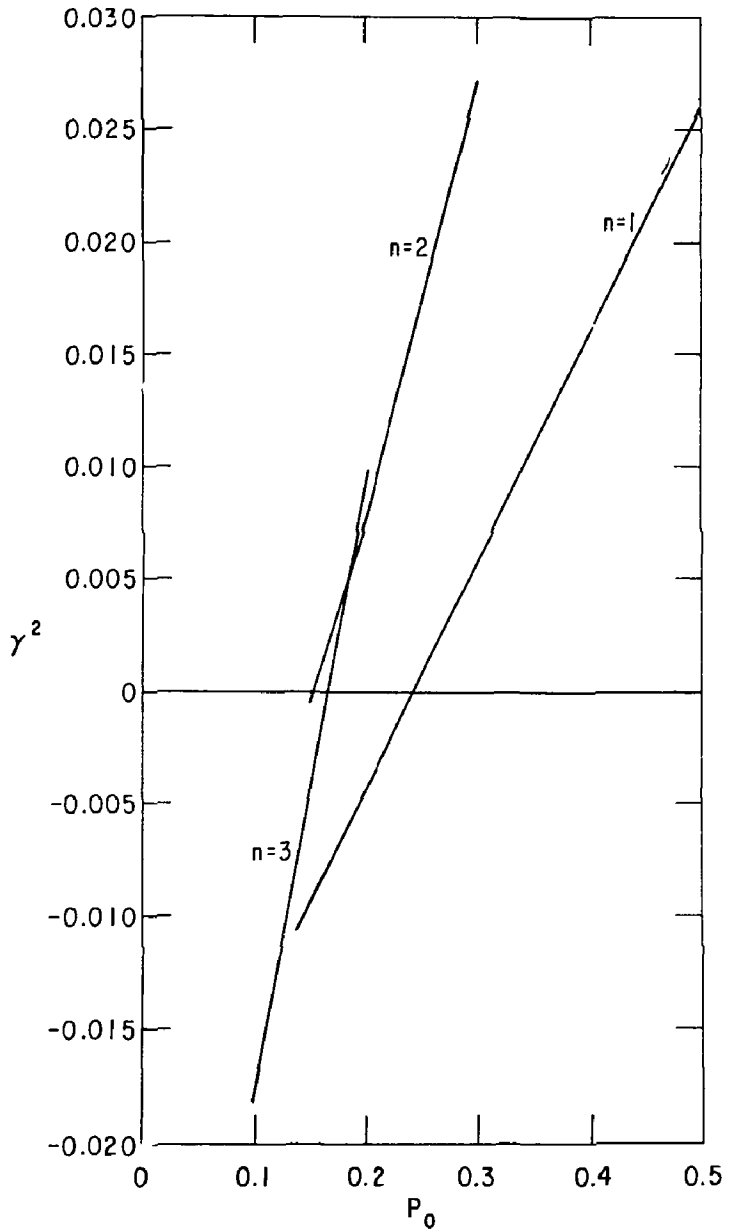

Fig. 12. (PPPL-802411)